Research Article

AC-YVAD-CMK Inhibits Pyroptosis and Improves Functional Outcome after Intracerebral Hemorrhage

Xiao Lin,[1,2] Haotuo Ye,[1,2] Felix Siaw-Debrah [iD],[1,2] Sishi Pan,[1,2] Zibin He,[1,2] Haoqi Ni,[1,2] Zhu Xu,[1,2] Kunlin Jin,[2] Qichuan Zhuge [iD],[1,2] and Lijie Huang [iD][1,2]

[1]*Department of Neurosurgery, The First Affiliated Hospital of Wenzhou Medical University, Wenzhou 325000, China*
[2]*Zhejiang Provincial Key Laboratory of Aging and Neurological Disorder Research, The First Affiliated Hospital of Wenzhou Medical University, Wenzhou 325000, China*

Correspondence should be addressed to Qichuan Zhuge; wyyyzhuge@163.com and Lijie Huang; lijiehuangwy@163.com

Intracerebral hemorrhage (ICH) refers to bleeding in the brain and is associated with the release of large amount of inflammasomes, and the activation of different cell death pathways. These cell death pathways lead to removal of inactivated and damaged cells and also result in neuronal cell damage. Pyroptosis is a newly discovered cell death pathway that has gained attention in recent years. This pathway mainly depends on activation of caspase-1-mediated cascades to cause cell death. We tested a well-known selective inhibitor of caspase-1, AC-YVAD-CMK, which has previously been found to have neuroprotective effects in ICH mice model, to ascertain its effects on the activation of inflammasomes mediated pyroptosis. Our results showed that AC-YVAD-CMK could reduce caspase-1 activation and inhibit IL-1β production and maturation, but has no effect on NLRP3 expression, an upstream inflammatory complex. AC-YVAD-CMK administration also resulted in reduction in M1-type microglia polarization around the hematoma, while increasing the number of M2-type cells. Furthermore, AC-YVAD-CMK treated mice showed some recovery of neurological function after hemorrhage especially at the hyperacute and subacute stage resulting in some degree of limb movement. In conclusion, we are of the view that AC-YVAD-CMK could inhibit pyroptosis, decrease the secretion or activation of inflammatory factors, and affect the polarization of microglia resulting in improvement of neurological function after ICH.

1. Introduction

Intracerebral hemorrhage (ICH) is a significant clinical emergency, which affects several million people worldwide [1]. ICH results in high mortality and morbidity and also causes serious disability and dependency throughout the world [2]. Over the years, many scientific researchers have focused on exploring potential mechanisms that may influence positively the outcome of ICH. The outcome of these studies has revealed targeting and attenuating increase release of proinflammatory cytokines, apoptosis, autophagy, and other cell death mechanisms around the hematoma region as major factors that influence the outcome [3, 4]. Recently, pyroptosis is another important cell death mechanism that has received much attention. The pyroptotic pathway consists of inflammasomes, which include apoptosis-associated speck-like proteins, caspase-recruiting domain (ASC), adapter protein,

and caspase-1, which is an inflammatory cysteine-aspartic proteinase [5]. This pathway, unlike apoptosis and autophagy, is mainly mediated by caspase-1 signaling pathway and is a cysteine aspartate protease-mediated programmed self-death [6, 7]. Activation of pyroptotic pathway not only activates inflammatory cytokines, but also induces cell death after proinflammatory intracellular content is released [5]. NLR protein-3 (NLRP3) inflammasome is a classic example of an inflammatory body. It consists of a variety of proteins including NLRP3, ASC, and caspase-1, which, when activated, breaks down caspase-1 into two subunits, p20 and p10. These subunits further activate the secretion or release of IL-1β and IL-18 [8]. Many experiments have confirmed caspase-1-mediated pyroptosis to be involved in various inflammatory processes [9] as well as many neurologically related diseases [10, 11]. It is therefore not surprising that NLRP3 inflammasome dependent inflammatory response has been

seen as a therapeutic target after intracerebral hemorrhage [12].

Microglia cells are considered resident immune cells of the central nervous system (CNS). In the mature brain, microglia cells maintain homeostasis and exist in a resting ramified state [13]. The progression and resolution of many CNS diseases are therefore dependent on the participation of activated microglia. While some microglial processes may be beneficial, microglia have also been shown to play a role in the secondary injury that occurs after ICH [14], as well as in other pathological processes of various neurological diseases, such as Alzheimer's disease, Parkinson's disease, and stroke [15–17]. Various studies have indicated that activated microglia have two main types, that is, M1 and M2. M1 is the classical pathway activation type, mainly secreting proinflammatory cytokines such as tumor necrosis factor-alpha (TNF-α), iNOS, and chemokine 2 and other molecules. The M2-type is a selective activation type and specifically expresses molecules such as CD206, CD68, and Arg-1 and releases interleukin 10(IL-10), transforming growth factor beta (TGF-β) and other molecules, which mainly plays a protective role against brain damage [13]. Although many studies have indicated that M1 microglia are activated during ICH episode leading to the progress of inflammatory reaction, others have also reported activation of M2 cell to protect brain from damage [18]. A clearer understanding into microglia polarization is still needed especially since little is known about the association between microglia and pyroptosis.

AC-TYR-VAL-ALA-ASP-CMK (AC-YVAD-CMK) is a well-known selective inhibitor of caspase-1 proven to have therapeutic effect on ischemic stroke [19], but the specific mechanism of action still remains unknown. Considering this known fact, we hypothesize that AC-YVAD-CMK could be used to treat collagenase induced ICH in mice model. We injected the drug into the mice brain and analyzed brain tissue for both inflammatory and anti-inflammatory protein expression and, at the same time, observed changes in mice behavior to explore the efficacy and potential mechanisms of drug.

2. Materials and Methods

2.1. Animals and Groups.
All clean grade male C57BL/6 mice with weight of 24-28g were purchased from the Shanghai Slaccas Experimental Animal Limited Liability Company (Shanghai, China). In a temperature-controlled room, mice were given food, water, and room light simulating normal day and night changes. The experiment was approved by the Animal Experimental Center of Wenzhou Medical University and was under its supervision.

Fifty-six mice were randomized into 4 different groups using computer-generated random numbers [20]: a normal group (normal, n = 14), a sham operation group (sham, n = 14), an intracerebral hemorrhage treated with vehicle group (ICH, n = 14), and an intracerebral hemorrhage treated with AC-YVAD-CMK group (ICH+T, n = 14). All the experimental proceedings were performed in a blinded manner.

2.2. ICH Model.
The collagenase injection method was used to induce intracerebral hemorrhage in experimental mice [21]. The mice were intraperitoneally anesthetized with 4% hydrochlorate (0.01 ml/g; Solarbio, Beijing, China) and fixed on the stereotactic head frame (Kopf Instruments, Tujunga, CA). Using a mini electric blanket to keep the rectal temperature at 37˚C ± 0.5˚C, the mice heads were shaved and a 1 cm long incision at the middle of the scalp was made, to expose mice skull. A 1 mm hole was drilled using a microdrill at 0.2 mm anterior to the bregma and 2.0 mm right to skull midline. Using a stereotactic 26-gauge needle inserted at about 3.7 mm deep in the right striatum, we injected collagenase VII-S (Sigma, C2399) into the brain using a microinfusion pump (KDS legato) at a concentration of 0.075U collagenase in 0.5 μl saline. The injection speed was constantly maintained at 2 μl/min by the microinfusion pump. Infusion needles were, however, left in place for 10 minutes and then removed at a rate of 1 mm/min after infusion was over. The sham group was, however, subjected to all surgical procedures but without collagenase infusion. Incision was sutured, and the mouse returned to its cage for recovery. In total, 3 experimental mice were recorded dead. Two mice died after injection of anesthesia (1 in each group, sham group and ICH+T group), with one dying from excessive injection of collagenase due to error in calibration of syringe pump. Mice were anesthetized and sacrificed after 24 h of ICH induction, and brain samples harvested. Samples obtained for the purpose of immunohistochemistry were stored in paraformaldehyde (40g/L) at 4˚C, whilst those for western blot were stored in liquid nitrogen after harvesting and later transferred to -80˚C storage (not more than 24 h before protein isolation).

2.3. Drug Injections.
As mentioned earlier [22], AC-YVAD-CMK was injected by intraventricular route, 15 minutes prior to collagenase injection. Preparation of AC-YVAD-CMK was done by dissolving solid AC-YVAD-CMK in DMSO and diluted further with phosphate buffer (PBS, final concentration DMSO = 0.1%) to a concentration of 400 ng/1 μL for every mouse. The drug was injected into the ventricle at a site 1 mm left and 2.5 mm ventral to the bregma. Vehicle group (ICH group) was injected with equal volume of vehicle (0.1%DMSO) before ICH. Sham group, however, had only needle insertion without any treatment protocol.

2.4. Western Blot Analysis.
Western blot was used to determine the amount of tissue protein expression as previously described [20]. A 2 mm thick coronal section of the ipsilateral hemisphere was collected from each group of specimens. Tissues were put into ice-cold radio-immunoprecipitation assay lysis buffer (RIPA) with phenylmethanesulfonyl fluoride (PMSF) (RIPA: PMSF=100:1) for 30 min and then crushed with tissue homogenizer. The homogenate was then transferred to a microtube and centrifuged at 12000 rad/min for 20 minutes in a precooled centrifuge at 4˚C. The BCA kit (Beyotime) was used to test the protein concentration. The protein of interest was separated by SDS-PAGE and then transferred to PVDF membrane, followed by blocking with 5% milk for 2 hours, and then incubated overnight with

primary antibodies, that is, caspase-1 (1:1000, ab1872, abcam, RRID:AB_302644), IL-1β (1:1000, abcam, RRID:AB_308765), cleaved-caspase-1 (1:500, ab1872, abcam, RRID:AB_302644), cleaved- IL1 beta (1:500, abcam, RRID:AB_308765), and GAPDH (1:1000, 5174S, Cell Signaling Technology, AB_10622025) at 4°C.After 24 hours; membranes were further incubated with secondary antibodies (1:5000) at room temperature for 1 hour. Band results were quantified using Image Lab software (Bio-Rad), and the target protein signals intensities were compared with β-actin or GAPDH intensity.

2.5. Brain Collection and Immunohistochemistry. Mice were anesthetized and sacrificed with 4% paraformaldehyde via transcardial perfusion. Brain tissues were quickly removed and fixed in 4% paraformaldehyde at 4°C for two days. After two days, tissues were fixed in 30% sucrose until they sank. The brain was embedded in O.C.T. Compound (SAKURA,4583) fixed on the frozen microtome and sliced to a thickness of 8 um. To determine the activation and polarization of microglia, immunofluorescent labeling using Iba1 labeled microglial, iNOS-labeled microglial M1, and CD206-labeled microglial M2 was done. As mentioned earlier, sections were soaked in paraformaldehyde and then rinsed with PBS. This was then blocked with 10% NDS (Normal Donkey Serum, dissolved in PBS) + 0.4% Triton-X for 1 hour, followed by incubation in antiserum to Iba1 (1:800, ab5076, Abcam, AB_2224402) and either iNOS (M1 marker; 1:300, ab15323, Abcam, AB_301857) or CD206 (M2 marker; 1:300, ab8918, Abcam, AB_306860) in 10% NDS + 0.4% Triton-X at 4°C for 12-16 hours. After 24 hr, sections were incubated with appropriate secondary antibodies conjugated to AlexaFluor-594 (Invitrogen, 1:300) and 488 (Invitrogen, 1:300). They were rinsed extensively in PBS +5% NDS for about 1 h and covered with DAPI (Vector Laboratories) for about 5 min. Sections were then examined using a scanning-fluorescence microscope (Leica Microsystems), at 40× objective, while image J software was used to determine colabeling between Iba1 with M1 or M2 markers. Statistical analysis from 6 randomly selected stained sections of brain tissue was done. Similarly, six digital micrographs at the marginal zone of the hematoma of each section were randomly taken. The numbers of double positive cells were selected, and the average of the slices of each brain was calculated (n = 3 for each group).

2.6. Neurologic Deficit. Each experimenter was blinded to all operational mice accessed for neurologic deficits with modified neurological severity score (mNSS) 7d after ICH. The tests included limb symmetry, exercise capability, balance ability, circling behavior, reflexes, and abnormal movements, with a maximum deficit score of 18 [23]. Before ICH, all mice were trained for three days.

2.7. Rotarod Test. Motor impairment was accessed using the rotarod test. The rotarod test was done as described previously [24]. Mice were trained for five consecutive days before ICH. The test, which lasted for 5 minutes, involves increasing the speed from 5 revolutions per minute (rpm) to 40 rpm, recording the time till the animal was felled from the
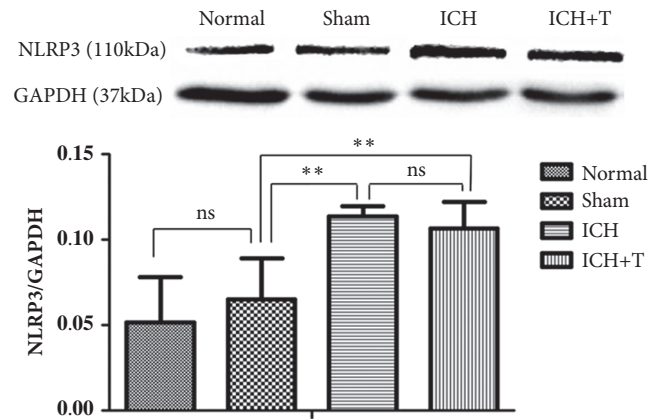

FIGURE 1: Protein levels were determined by western blotting. NLRP3 levels showed no obvious changes between ICH and ICH+T group, with similar observation between normal and sham group. However, there was significant difference between sham group and both ICH and ICH+T group, (∗∗P <0.01, ns=no significance). n=4 for each group. One-way ANOVA.

drum (in seconds). After training, if the experimental animal could not last for about 250s on the instrument, they were excluded from the experiment. Each session included three training sessions, with each lasting about 300 seconds. The next training is done on an average interval of 20 minutes. The final calculation involves taking the average of the three. In this study, all experimental mice were able to meet the requirements after training.

2.8. Statistical Analyses. The statistical analysis of the experimental data was done using SPSS 22.0 software and Prism 5.0. All time related results were expressed as means ± standard deviation (SD). One-way ANOVA was used in western blot and immunohistochemistry. For neurologic deficit and rotarod test, repeated measures ANOVA analysis and two-way ANOVA were used to determine the difference between groups. Results were only considered to be statistically significant at P < 0.05.

3. Results

3.1. AC-YVAD-CMK Had No Effects on NLRP3 Inflammasome after ICH. Western blot analyses showed increased NLRP3 protein expression in ICH group and ICH+T group compared with normal and sham group. However, there was no significant change between ICH group and ICH+T group (Figure 1).

3.2. AC-YVAD-CMK Inhibited Caspase-1 Activation and Reduced the Amount of Mature IL-1β after ICH. Western blot analyses showed that caspase-1 continued to increase 24 hours after ICH in ICH group compared with the sham group. However, activation was significantly inhibited in AC-YVAD-CMK-treated mice compared with untreated mice. The ratio of activated caspase-1 to precursors showed a significant decrease (Figure 2). After 24 hours of ICH an increased expression ofIL-1β and mature-IL-1β was observed.
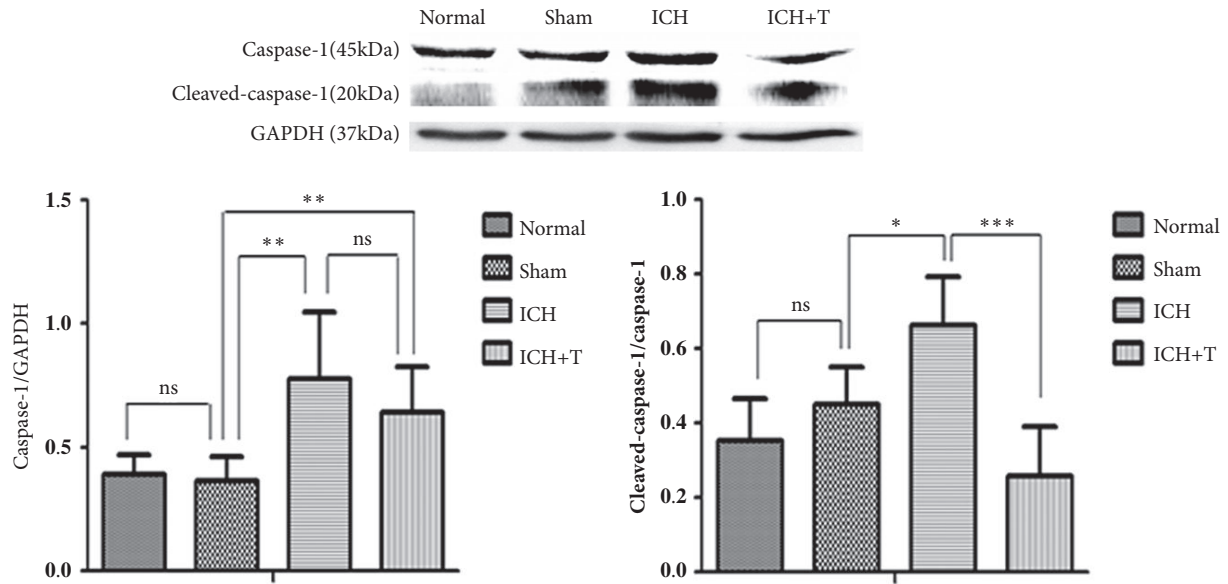
FIGURE 2: Caspase-1 expression by western blot. Sham group compared with the normal group showed no obvious difference between caspase-1 and cleaved-caspase-1/caspase-1 expression. However, compared with the sham group, both caspase-1 and cleaved-caspase-1/caspase-1 showed significant increase after ICH. ICH+T group also showed lower expression of caspase-1 compared with ICH group (∗P <0.05, ∗∗P<0.01, ∗ ∗ ∗P<0.001, ns=no significance), n=4 for each group. One-way ANOVA.
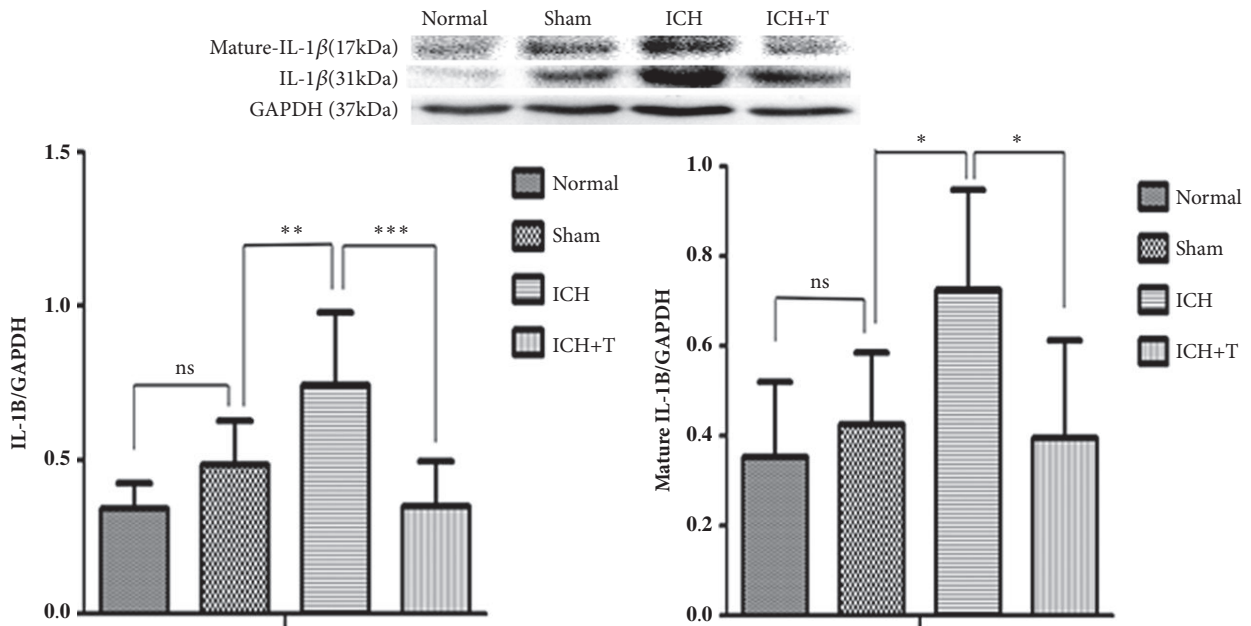

FIGURE 3: IL-1β expression by western blot. There was no significant difference between normal and sham group. Expression of IL-1β and mature IL-1β increased compared to the sham group after ICH. The ICH+T group showed decrease expression of IL-1β and mature IL-1β as compared to ICH group (∗P <0.05, ∗∗P<0.01). (∗ ∗ ∗P <0.001∗∗P <0.01, ∗P<0.05, ns=no significance). n=4 for each group. One-way ANOVA.

Pretreatment with AC-YVAD-CMK, however, reduced the production of IL-1β and mature-IL-1β (Figure 3).

3.3. AC-YVAD-CMK Decreased the Activation of M1 Microglial and Increased M2 Microglial Cells.
To determine the activation state of microglia after ICH, we collected mouse brain slices, and sections were colabeled with Iba1 and either M1 markers (iNOS) or M2 markers (CD206). Confocal analysis showed that Ac-YVAD-CMK could significantly decrease the double positive cell ratio of iNOS+/Iba1+ cells surrounding the hematoma 1 day after ICH (Figure 4). The costaining CD206/Iba1 analyses showed that CD206+/Iba1+ cells increased markedly in the ICH+T group as compared to ICH group (Figure 5). In summary, the results show that
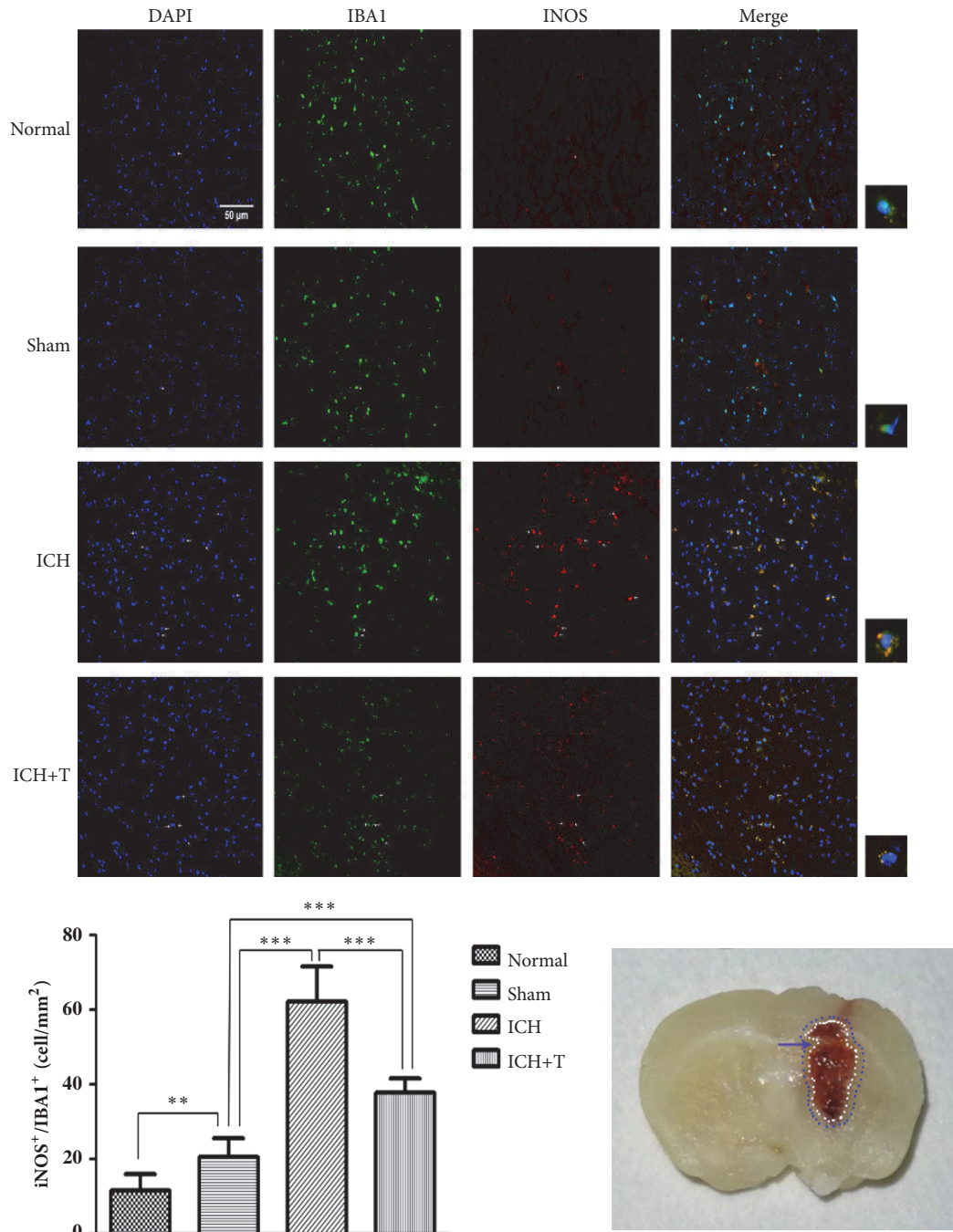
FIGURE 4: AC-YVAD-CMK decreased iNOS+/Iba1+ cells. ICH group showed increased iNOS+/Iba1+ cells 1 day after ICH as compared to the sham group. ICH+T, however, showed significantly decreased iNOS+/Iba1+ cells 1 day after ICH group compared with ICH group. Arrows indicate iNOS+/Iba1+ cells ($**P < 0.01, ***P < 0.001$, n = 3). ICH+T: treated with AC-YVAD-CMK. ICH: treated with DMSO. The region between the red and blue cycle (blue arrow) indicates the area around hematoma, where images were taken. Scale bar= 50 μm. (The white arrow in immunofluorescence staining picture indicates the stained area; the white square shows the costained cells, which is the enlarged part.) One-way ANOVA.

pretreatment with Ac-YVAD-CMK can inhibit activation of M1 microglial and can also enhance M2 microglial activation after ICH.

3.4. AC-YVAD-CMK Improved Neurological Behavior after ICH. The normal group had 0 score and, as such, were not placed on the figure. The sham group did not show any neurological dysfunction after surgery. An obvious functional deficit was exhibited in ICH group 7d after ICH. ICH group compared with the sham group shows significant functional impairment. The modified neurological severity score (mNSS) assessment showed no effects of vehicle in
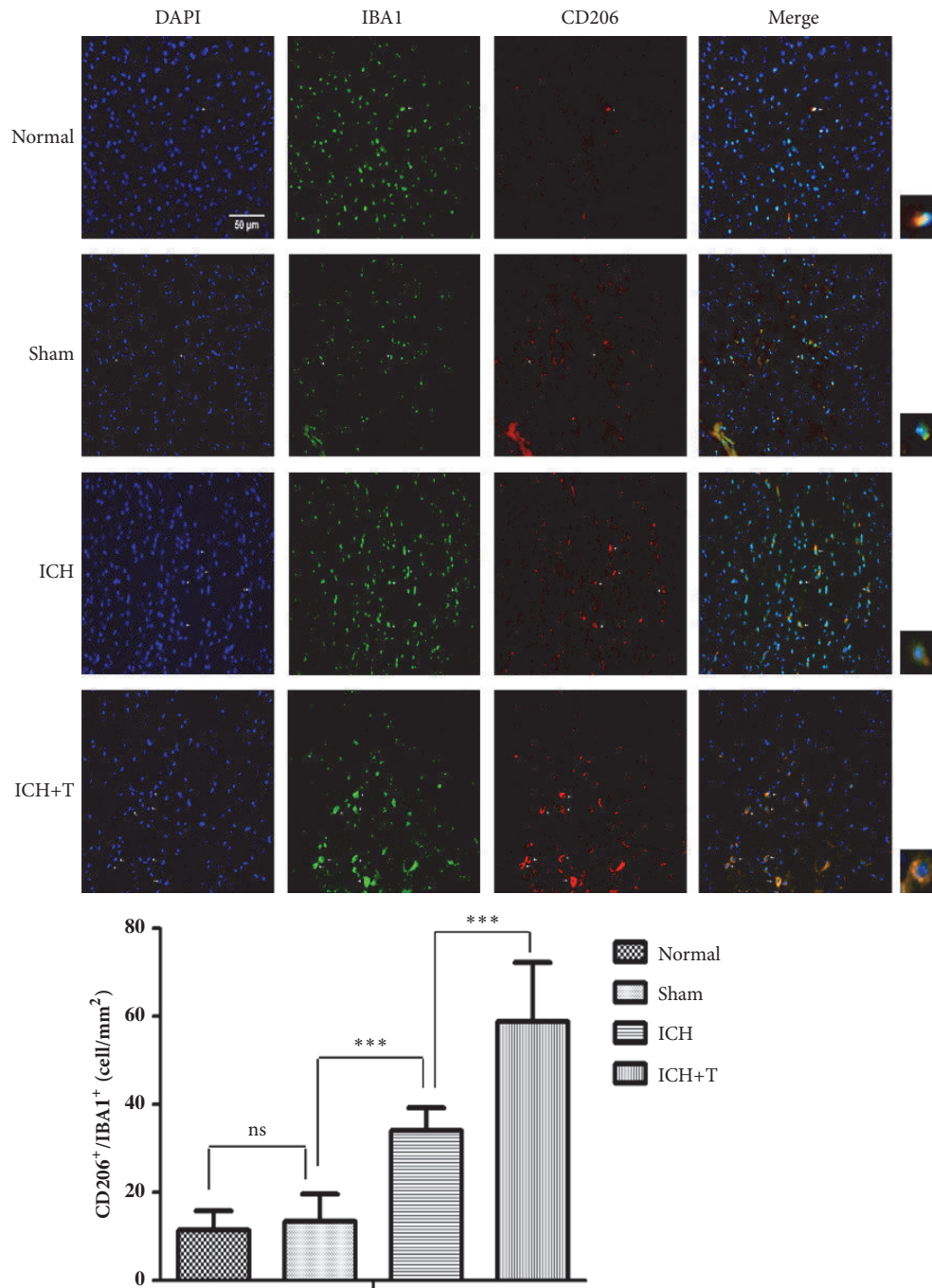
FIGURE 5: AC-YVAD-CMK increased CD206+/Iba1+ cells. ICH group compared with sham group showed increased CD206+/Iba1+ cells 1 day after ICH. ICH+T group compared with ICH group also demonstrated significant increase in CD206+/Iba1+ cells. Arrows indicate CD206+/Iba1+ cells ($***P < 0.001$, n = 3). ICH+T: treated with AC-YVAD-CMK. ICH: treated with DMSO. Scale bar= 50 μm. One-way ANOVA.

the vehicle group, while ICH+T group showed significant improvement in neurological function (Figure 6). This difference first appeared in the sixth hour after ICH and then after seven days.

3.5. AC-YVAD-CMK Improved the Result of Rotarod Test. As described earlier, different groups used the same acceleration method. The duration of the test results of the normal group mice is greater than 300s; it was not shown in the figure. In the sham group, mice were found not to have neurological deficits in the rotarod test, but ICH mice showed severe neurological deficits following surgery. After treatment with AC-YVAD-CMK, mice showed significant improvement of motor impairment compared with ICH group (Figure 7), n=6 for each group.
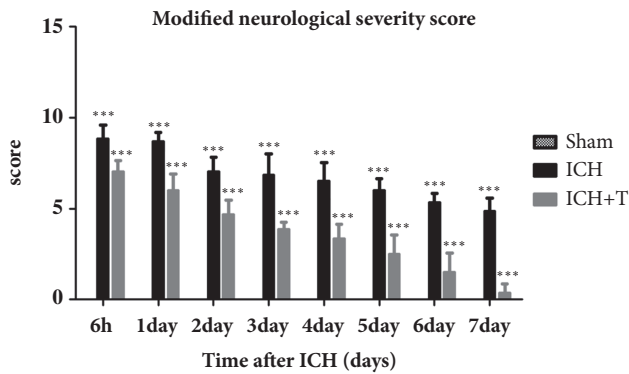
FIGURE 6: The sham group did not show any neurological dysfunction after surgery. The mNSS score of ICH group was significantly higher than sham group seven days after ICH ($***P<0.001$). Pretreatment with Ac-YVAD-CMK improved modified neurological severity score 7 days after ICH. mean ± SD, Two-way ANOVA. The treatment group in comparison with the ICH group showed significant difference, and interaction was obvious between the treatment method and the test time; repeated measure ANOVA; n=6 for each group ($***P<0.001$). ICH+T: treated with Ac-YVAD-CMK. ICH: treated with DMSO.
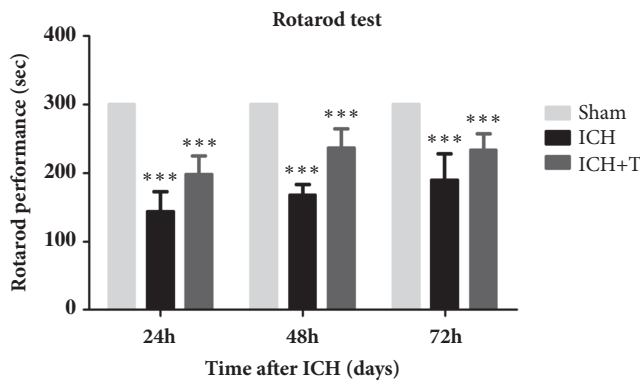

FIGURE 7: The sham group did not change in rotarod performance after surgery. The duration of the ICH mice decreased significantly compared with the sham group after 72 h of ICH ($*** P<0.001$). AC-YVAD-CMK treatment improved rotarod performance time after 72 hrs as compared with ICH group ($*** P<0.001$, $** P<0.01$). mean ± SD, Two-way ANOVA. Significant difference was established between the ICH and treatment group; however, there was no interaction between the treatment method and the test time; repeated measure ANOVA; n=6 for each group. ICH+T: treated with Ac-YVAD-CMK. ICH: treated with DMSO.

4. Discussion

During an episode of acute intracerebral hemorrhage, many inflammatory cascades are triggered around the hematoma area leading to the release of cytokines and the breakdown of the blood-brain barrier. These factors together with other inflammatory factors further aggravate the migration of systemic inflammatory cells to the hematoma area [25, 26]. NLRP3 inflammasome is widely studied and accepted to play a crucial role in the inflammatory process in the nervous system, especially after ICH [12].

NLRP3 plays an important role in the initial process of pyroptosis during an ICH episode. This is demonstrated in the elevation of NLRP3 inflammasome expression and activation of caspase-1 after ICH. AC-YVAD-CMK is a well-known specific inhibitor of caspase-1. However, whether AC-YVAD-CMK exerts inhibitory effect on the expression of NLRP3 after ICH is still unknown. In this study, we discovered increased NLRP3 expression after ICH and at the same time, we noticed increased caspase-1 activation, which was probably induced by NLRP3 inflammasome. Administration of AC-YVAD-CMK was seen to attenuate caspase-1 activation. However, there is no evidence suggested effect on the expression of NLRP3. AC-YVAD-CMK administration led to decreased levels of inflammation as well as pyroptosis. Because pyroptotic cell death depends on caspase-1 activation, AC-YVAD-CMK administration may have, therefore, attenuated caspase -1 activation, hence inhibiting caspase-1-mediated pyroptotic cell death.

Our experiment used a suitable dosage of 400 ng of AC-YVAD-CMK according to the results of Hideaki's study for ischemic neuronal damage [19]. This was due to the fact that dosages greater than 800 ng per mice led to the death of mice, whereas the dosages less than 200 ng had no significant effect. We, therefore, used a dosage of 400 ng as our optimum dosage throughout our experiment. In this study, results showed that activated NLRP3 inflammasome, including NLRP3, caspase-1, as well as activated cleaved-caspase-1 (p20) and IL-1β, had increased expression in ICH mice. A comparison between the ICH induced group and the control showed increased expression of NLRP3 and caspase-1, and an increased level of circulating IL-1β. This was probably due to the triggered activation of NLRP3 inflammasome pathway, which aggravates the release of IL-1β. Mice administrated with AC-YVAD-CMK, on the other hand, showed the reverse with significant reduction of caspase-1 expression, downregulating the mature IL-1β. These results indicate that NLRP3 inflammasome is most likely activated during an ICH episode leading to NLRP3-induced caspase-1 dependent inflammatory response. Therefore, targeted inhibition of caspase-1 activation or NLRP3 inflammasome activation may serve as a potential new therapeutic target for inhibiting the pyroptosis after ICH.

Microglia, innate immune cells of the central nervous system, occupy a very important position in the occurrence and progression of nervous system diseases. Recent studies have shown that M1-signature (proinflammatory) cytokines significantly rise after ICH. For example, activated nuclear factor-κB (NF-κB) was seen to migrate into the nucleus at 13–48 h after ICH and at the same time, IL-1β and tumor necrosis factor (TNF) levels increased within 1 day after ICH, while downregulation of TNF-α expression was associated with reduction in hematoma volume [27–29]. Some researchers found that M1 markers such as CD16, CD32, and iNOS are highly expressed on microglia on days 1 and 3 after ICH [30], suggesting that M1 cells' polarization occurs early in the acute phase. M2-type microglia are considered to be protective cells. Induction of microglia M2 polarization is considered to be beneficial against damaged brain from nervous system injury disease like ischemic and spinal cord

injury [31, 32]. This study found that IL-4 administration can promote M2 polarization and reduce ischemic lesion volume, and lipopolysaccharide preconditioning improves spinal cord injury by facilitating M2 activation. Similarly, the resolution of hematoma volume was seen to be strongly associated with selective activation of M2 microglia, which promoted phagocytosis [33]. Recent experimental findings have indicated that M1 polarization of microglia will increase after ICH evident by an increase in interleukin 1-beta (IL-1β) secretion [34]. Another study found that NLRP3 is mainly concentrated in astrocytes and microglia in the CNS [35, 36]; as such, the production of NLRP3 and IL-1β is, therefore, associated with microglia activation to some extent. Our study found that pretreatment of ICH model with AC-YVAD-CMK could inhibit the activation of caspase-1 and reduce the production and maturation of IL-1β without affecting NLRP3. Therefore, we hypothesized that AC-YVAD-CMK might have affected the microglia changes around the hematoma. In order to prove whether the microglial cells around the hematoma after ICH were changed, we performed immunofluorescence staining from frozen sections of mouse brain tissue, for which results showed significant microglia activation around the hematoma especially that of M1 microglia. It was shown that M1 microglia increased significantly in the surrounding area after ICH, while M2 microglia only slightly increased. This result is consistent with the findings of other researchers who studied changes in microglia after ICH [37]. The main effect of microglial activation and polarization after ICH is the release of inflammatory cytokines and phagocytic debris [14]. However, the effect after pretreatment with AC-YVAD-CMK resulted in significant decrease in M1 polarization, more prominent after ICH 24 h, whereas the proportion of M2 cells increased. This shows that mice with AC-YVAD-CMK treatment showed signs of microglia polarization from M1 to M2 around the hematoma region favoring the migration of more M2 to this region. M2 microglial cells have been proved to possess a neural repair effect. It can secrete anti-inflammatory cytokines and increase neuroprotective factors in the central nervous system [34]. Therefore, we are of the view that this change in microglia polarization favoring M2 microglia may be the key to improving neurological impairment after ICH. Although the mechanism of this change is still unknown to us, further research is needed to help explain this phenomenon. In addition, changes in the expression of the pyroptotic proteins and the changes in the bound microglia suggest that microglia in the brain had M1-type polarization after ICH, which resulted in a large number of NLRP3 inflammasomes and caspase-1 activation leading to subsequent release of IL-1β and pyroptotic response. With treatment of AC-YVAD-CMK, the activation of caspase-1 was blocked, which prevented the release of subsequent inflammatory factors and, at the same time, promoted the transformation of microglia into M2-type, exerting anti-inflammatory effects, leading to improved neurological function.

From our results, we deduced that AC-YVAD-CMK could inhibit pyroptosis by inhibiting the expression and activation of other inflammatory factors and also change the polarization state of microglia. This positive effect was seen in the AC-YVAD-CMK pretreatment group demonstrated by the improvement in neurological function as recorded by mNSS and rotarod test. We discovered that the drug treated group showed significant improvement after ICH mainly due to the attenuation of further injury due to aggravated inflammation. Our assumption is that AC-YVAD-CMK improves nerve function by inhibiting pyroptosis and providing neuroprotection after acute ICH episode. Furthermore, we found that administration of AC-YVAD-CMK not only improved neurological impairment, but also improved limb mobility and fatigue tolerance after ICH. In conclusion, we hypothesize that AC-YVAD-CMK improving neurological function may be related to its inhibition of pyroptosis and promotion of microglial cell polarization to M2-type, so it gives an anti-inflammatory effect. In addition, AC-YVAD-CMK have been shown to reduce brain edema at 24H and 72H after ICH [38]. But whether it can affect the change of cerebral hematoma volume is unknown. We will examine it in subsequent experiments.

Not until recently have many researchers thought that there was no difference between pyroptosis and apoptosis. However, animal studies of intracerebral hemorrhage have discovered the presence of apoptotic cells in brain tissue 6 h after injection of autologous blood, which was accompanied by higher caspase-3 gene expression [39]. In another experiment, apoptosis was seen to be mediated by caspase protease, but with caspase-3 as its key enzyme [31]. Ferroptosis is a newly discovered cell death pathway in recent years. Discovered by Dixon, ferroptosis is characterized by the overwhelming, iron-dependent accumulation of lethal lipid ROS. This requirement for ROS accumulation appears to be universal. In some cell studies, NOX-family enzymes make important contributions to this process [40]. It is well known that there is a large amount of iron accumulation after ICH, so whether ferroptosis is involved in aggravating effect of ICH is a new direction of investigation. Recent studies on ferroptosis have reported that the administration of ferrostatin-1, a known specific inhibitor of ferroptosis, resulted in the prevention of neuronal death after ICH. Ferrostatin-1 was documented to reduce iron deposition induced by hemoglobin in experimental ICH mice, thereby promoting neurologic function recovery, indicating the likely role of ferroptosis in the disease process of ICH [41]. In contrast to earlier mentioned cell death pathways, pyroptosis is mainly dependent on caspase-1 and not caspase-3 pathway, although the specific mechanism remains unclear. At present, there are many studies on the detection of the expression of signal molecules such as NLRP3, caspase-1, IL-1β, and IL-18; however, these studies are at the ex vivo level. Other studies have identified Gasdermin D (GSDMD) protein to be also involved in pyroptosis, with the exact mechanism still being undiscovered. These studies used chemotherapy drugs to activate caspase-3, which led to the cleavage of GSDME and subsequent pyroptosis. However, it was believed that caspase-3 led to apoptosis, which began the process of pyroptosis, but not direct involvement of caspase-3 in the pyroptosis. [42]. There is still much controversy about the role of pyroptosis in the CNS disease; that is, whether pyroptosis is beneficial or harmful in the disease and causing process is yet to be

determined. Different diseases may have different outcomes, with the same disease having different effects at different stages of its development. In addition, whether pyroptosis has a role in tumor diseases [43, 44] is yet to be ascertained. Although the role of pyroptosis in different diseases and its signal pathways is still not very clear at present, with the gradual acceptance of pyroptosis by people, study on its specific effects and molecular mechanisms will surely bring new therapeutic methods and therapeutic targets for the treatment of diseases.

5. Conclusions

In summary, AC-YVAD-CMK, a well-known caspase-1 inhibitor, reduces brain damage caused by ICH in mice. This protective effect could be as a result of the inhibition of inflammatory signaling activation, attenuation of pyroptosis, and influence of microglial polarization. Preventing cleavage of caspase-1 into activated form by Ac-YVAD-CMK could, therefore, be a new way to prevent or attenuate inflammation and neurological injury after ICH.

Data Availability

The data used to support the findings of this study are available from the corresponding author upon request.

Conflicts of Interest

There are no conflicts of interest to declare.

Authors' Contributions

All authors had full access to all the data in the study and take responsibility for the integrity of the data and the accuracy of the data analysis. Study concept and design are done by Xiao Lin, Qichuan Zhuge, Lijie Huang, and Kunlin Jin. Acquisition of data is done by Xiao Lin, Haotuo Ye, and Felix Siaw-Debrah. Analysis and interpretation of data are done by Xiao Lin and Sishi Pan. Drafting of the manuscript is done by Xiao Lin and Felix Siaw-Debrah. Critical revision of the manuscript for important intellectual content is done by Qichuan Zhuge and Lijie Huang. Statistical analysis is done by Haoqi Ni and Zhu Xu.

Acknowledgments

References

[1] E. J. Benjamin, S. S. Virani, C. W. Callaway et al., "Heart Disease and Stroke Statistics-2018 Update: A Report From the American Heart Association," *Circulation*, vol. 137, no. 12, pp. e67–e492, 2018.

[2] C. J. van Asch, M. J. Luitse, G. J. Rinkel, I. van der Tweel, A. Algra, and C. J. Klijn, "Incidence, case fatality, and functional outcome of intracerebral haemorrhage over time, according to age, sex, and ethnic origin: a systematic review and meta-analysis," *The Lancet Neurology*, vol. 9, no. 2, pp. 167–176, 2010.

[3] A. Simi, N. Tsakiri, P. Wang, and N. J. Rothwell, "Interleukin-1 and inflammatory neurodegeneration," *Biochemical Society Transactions*, vol. 35, no. 5, pp. 1122–1126, 2007.

[4] C. M. Smith, Y. Chen, M. L. Sullivan, P. M. Kochanek, and R. S. B. Clark, "Autophagy in acute brain injury: feast, famine, or folly?" *Neurobiology of Disease*, vol. 43, no. 1, pp. 52–59, 2011.

[5] T. Bergsbaken, S. L. Fink, and B. T. Cookson, "Pyroptosis: host cell death and inflammation," *Nature Reviews Microbiology*, vol. 7, no. 2, pp. 99–109, 2009.

[6] Y. Chen, M. R. Smith, K. Thirumalai, and A. Zychlinsky, "A bacterial invasin induces macrophage apoptosis by binding directly to ICE," *EMBO Journal*, vol. 15, no. 15, pp. 3853–3860, 1996.

[7] D. Hersh, D. M. Monack, M. R. Smith, N. Ghori, S. Falkow, and A. Zychlinsky, "The Salmonella invasin SipB induces macrophage apoptosis by binding to caspase-1," *Proceedings of the National Acadamy of Sciences of the United States of America*, vol. 96, no. 5, pp. 2396–2401, 1999.

[8] T. Horng, "Calcium signaling and mitochondrial destabilization in the triggering of the NLRP3 inflammasome," *Trends in Immunology*, vol. 35, no. 6, pp. 253–261, 2014.

[9] L. Danelishvili and L. E. Bermudez, "Analysis of pyroptosis in bacterial infection," *Methods in Molecular Biology*, vol. 1004, pp. 67–73, 2013.

[10] M. S. Tan, L. Tan, T. Jiang, X. C. Zhu, H. F. Wang, and C. D. Jia, "Amyloid-beta induces NLRP1-dependent neuronal pyroptosis in models of Alzheimer's disease," *Cell death & disease*, vol. 5, p. e1382, 2014.

[11] W. Chang, J. Lin, J. Dong, and D. Li, "Pyroptosis: An inflammatory cell death implicates in atherosclerosis," *Medical Hypotheses*, vol. 81, no. 3, pp. 484–486, 2013.

[12] Q. Ma, S. Chen, Q. Hu, H. Feng, J. H. Zhang, and J. Tang, "NLRP3 inflammasome contributes to inflammation after intracerebral hemorrhage," *Annals of Neurology*, vol. 75, no. 2, pp. 209–219, 2014.

[13] J. A. Kabba, Y. Xu, H. Christian et al., "Microglia: Housekeeper of the Central Nervous System," *Cellular and Molecular Neurobiology*, vol. 38, no. 1, pp. 53–71, 2018.

[14] R. A. Taylor and L. H. Sansing, "Microglial responses after ischemic stroke and intracerebral hemorrhage," *Clinical and Developmental Immunology*, vol. 2013, Article ID 746068, 10 pages, 2013.

[15] G. Szalay, B. Martinecz, N. Lénárt et al., "Microglia protect against brain injury and their selective elimination dysregulates neuronal network activity after stroke," *Nature Communications*, vol. 7, Article ID 11499, 2016.

[16] C. Ghadery, Y. Koshimori, S. Coakeley et al., "Microglial activation in Parkinson's disease using [18F]-FEPPA," *Journal of Neuroinflammation*, vol. 14, no. 1, 2017.

[17] C. Condello, P. Yuan, and J. Grutzendler, "Microglia-Mediated Neuroprotection, TREM2, and Alzheimer's Disease: Evidence From Optical Imaging," *Biological Psychiatry*, 2017.

[18] X.-Y. Xiong, L. Liu, and Q.-W. Yang, "Functions and mechanisms of microglia/macrophages in neuroinflammation and neurogenesis after stroke," *Progress in Neurobiology*, vol. 142, pp. 23–44, 2016.

[19] H. Hara, R. M. Friedlander, V. Gagliardini et al., "Inhibition of interleukin 1b converting enzyme family proteases reduces ischemic and excitotoxic neuronal damage," *Neurobiology*, vol. 94, pp. 2007–2012, 1997.

[20] C.-H. Wu, C.-C. Chen, C.-Y. Lai et al., "Treatment with TO901317, a synthetic liver X receptor agonist, reduces brain damage and attenuates neuroinflammation in experimental intracerebral hemorrhage," *Journal of Neuroinflammation*, vol. 13, no. 1, 2016.

[21] P. R. Krafft, W. B. Rolland, K. Duris et al., "Modeling intracerebral hemorrhage in mice: Injection of autologous blood or bacterial collagenase," *Journal of Visualized Experiments*, no. 67, 2012.

[22] K. P. Doyle, T. Yang, N. S. Lessov et al., "Nasal administration of osteopontin peptide mimetics confers neuroprotection in stroke," *Journal of Cerebral Blood Flow & Metabolism*, vol. 28, no. 6, pp. 1235–1248, 2008.

[23] W. Jiang, G. Liang, X. Li et al., "Intracarotid transplantation of autologous adipose-derived mesenchymal stem cells significantly improves neurological deficits in rats after MCAo," *Journal of Materials Science: Materials in Medicine*, vol. 25, no. 5, pp. 1357–1366, 2014.

[24] K.-H. Choi, M.-S. Park, H.-S. Kim et al., "Alpha-lipoic acid treatment is neurorestorative and promotes functional recovery after stroke in rats," *Molecular Brain*, vol. 8, no. 1, article no. 9, 2015.

[25] M. C. Loftspring, J. McDole, A. Lu, J. F. Clark, and A. J. Johnson, "Intracerebral hemorrhage leads to infiltration of several leukocyte populations with concomitant pathophysiological changes," *Journal of Cerebral Blood Flow & Metabolism*, vol. 29, no. 1, pp. 137–143, 2009.

[26] A. Manaenko, H. Chen, J. H. Zhang, and J. Tang, "Comparison of different preclinical models of intracerebral hemorrhage," in *Intracerebral Hemorrhage Research: From Bench to Bedside*, J. Zhang and A. Colohan, Eds., vol. 111 of *Acta Neurochirurgica Supplementum*, pp. 9–14, 2011.

[27] Z. Zhang, Y. Liu, Q. Huang et al., "NF-κB activation and cell death after intracerebral hemorrhage in patients," *Neurological Sciences*, vol. 35, no. 7, pp. 1097–1102, 2014.

[28] H. Wu, Z. Zhang, X. Hu et al., "Dynamic changes of inflammatory markers in brain after hemorrhagic stroke in humans: A postmortem study," *Brain Research*, vol. 1342, pp. 111–117, 2010.

[29] J. Wang and S. E. Tsirka, "Contribution of extracellular proteolysis and microglia to intracerebral hemorrhage," *Neurocritical Care*, vol. 3, no. 1, pp. 77–85, 2005.

[30] X. Lan, X. Han, Q. Li et al., "Pinocembrin protects hemorrhagic brain primarily by inhibiting toll-like receptor 4 and reducing M1 phenotype microglia," *Brain, Behavior, and Immunity*, vol. 61, pp. 326–339, 2017.

[31] X. Zhao, H. Wang, G. Sun, J. Zhang, N. J. Edwards, and J. Aronowski, "Neuronal interleukin-4 as a modulator of microglial pathways and ischemic brain damage," *The Journal of Neuroscience*, vol. 35, no. 32, pp. 11281–11291, 2015.

[32] K. Hayakawa, R. Okazaki, K. Morioka, K. Nakamura, S. Tanaka, and T. Ogata, "Lipopolysaccharide preconditioning facilitates M2 activation of resident microglia after spinal cord injury," *Journal of Neuroscience Research*, vol. 92, no. 12, pp. 1647–1658, 2014.

[33] X. Lan, X. Han, Q. Li, Q.-W. Yang, and J. Wang, "Modulators of microglial activation and polarization after intracerebral haemorrhage," *Nature Reviews Neurology*, vol. 13, no. 7, pp. 420–433, 2017.

[34] Z. Zhang, Z. Zhang, H. Lu, Q. Yang, H. Wu, and J. Wang, "Microglial polarization and inflammatory mediators after intracerebral hemorrhage," *Molecular Neurobiology*, 2016.

[35] M. D. Weber, M. G. Frank, K. J. Tracey, L. R. Watkins, and S. F. Maier, "Stress induces the danger-associated molecular pattern HMGB-1 in the hippocampus of male sprague dawley rats: a priming stimulus of microglia and the NLRP3 inflammasome," *The Journal of Neuroscience*, vol. 35, no. 1, pp. 316–324, 2015.

[36] Y. Pan, X.-Y. Chen, Q.-Y. Zhang, and L.-D. Kong, "Microglial NLRP3 inflammasome activation mediates IL-1β-related inflammation in prefrontal cortex of depressive rats," *Brain, Behavior, and Immunity*, vol. 41, no. 1, pp. 90–100, 2014.

[37] J. Yang, S. Ding, W. Huang et al., "Interleukin-4 ameliorates the functional recovery of intracerebral hemorrhage through the alternative activation of microglia/macrophage," *Frontiers in Neuroscience*, vol. 10, article no. 61, 2016.

[38] B. Wu, Q. Ma, N. Khatibi et al., "Ac-YVAD-CMK Decreases Blood-Brain Barrier Degradation by Inhibiting Caspase-1 Activation of Interleukin-1β in Intracerebral Hemorrhage Mouse Model," *Translational Stroke Research*, vol. 1, no. 1, pp. 57–64, 2010.

[39] C. Gong, N. Boulis, J. Qian, D. E. Turner, J. T. Hoff, and R. F. Keep, "Intracerebral hemorrhage-induced neuronal death," *Neurosurgery*, vol. 48, no. 4, pp. 875–883, 2001.

[40] S. J. Dixon, K. M. Lemberg, M. R. Lamprecht et al., "Ferroptosis: an iron-dependent form of nonapoptotic cell death," *Cell*, vol. 149, no. 5, pp. 1060–1072, 2012.

[41] Q. Li, X. Han, X. Lan et al., "Inhibition of neuronal ferroptosis protects hemorrhagic brain," *JCI Insight*, vol. 2, no. 7, 2017.

[42] W. T. He, H. Wan, L. Hu et al., "Gasdermin D is an executor of pyroptosis and required for interleukin-1beta secretion," *Cell research*, vol. 25, no. 12, pp. 1285–12898, 2015.

[43] J. Dupaul-Chicoine, A. Arabzadeh, M. Dagenais et al., "The Nlrp3 Inflammasome Suppresses Colorectal Cancer Metastatic Growth in the Liver by Promoting Natural Killer Cell Tumoricidal Activity," *Immunity*, vol. 43, no. 4, pp. 751–763, 2015.

[44] V. Derangère, A. Chevriaux, F. Courtaut et al., "Liver X receptor β activation induces pyroptosis of human and murine colon cancer cells," *Cell Death & Differentiation*, vol. 21, no. 12, pp. 1914–1924, 2014.